

Teacher-Guided Causal Interventions for Image Denoising: Orthogonal Content-Noise Disentanglement in Vision Transformers

Kuai Jiang¹, Zhaoyan Ding¹, Guijuan Zhang², Dianjie Lu² and Zhuoran Zheng³

¹China University of Mining and Technology

²Shandong Normal University

³Qilu University of Technology

{kuaijiang, dingzhaoyan}@cumt.edu.cn, {zhangguijuan, ludianjie}@sdnu.edu.cn, zhengzr@njust.edu.cn

Abstract

Conventional image denoising models often inadvertently learn spurious correlations between environmental factors and noise patterns. Moreover, due to high-frequency ambiguity, they struggle to reliably distinguish subtle textures from stochastic noise, resulting in over-removed details or residual noise artifacts. We therefore revisit denoising via causal intervention, arguing that purely correlational fitting entangles intrinsic content with extrinsic noise, which directly degrades robustness under distribution shifts. Motivated by this, we propose the Teacher-Guided Causal Disentanglement Network (TCD-Net), which explicitly decomposes the generative mechanism via structured interventions on feature spaces within a Vision Transformer framework. Specifically, our method integrates three key components: (1) An Environmental Bias Adjustment (EBA) module projects features into a stable, de-centered subspace to suppress global environmental bias (de-confounding). (2) A dual-branch disentanglement head employs an orthogonality constraint to force a strict separation between content and noise representations, preventing information leakage. (3) To resolve structural ambiguity, we leverage Nano Banana Pro, Google’s reasoning-guided AI image generation model, to guide a causal prior, effectively pulling content representations back onto the natural-image manifold. Extensive experiments demonstrate that TCD-Net outperforms mainstream methods across multiple benchmarks in both fidelity and efficiency, achieving a real-time speed of 104.2 FPS on a single RTX 5090 GPU.

1 Introduction

Image denoising is a fundamental step in computational photography and low-level vision, serving as a prerequisite for downstream perception and prediction. Yet, denoising remains intrinsically ill-posed: the observation is jointly shaped by intrinsic scene content and extrinsic corruption sources (e.g., sensor noise, ISP pipelines, illumination), while both

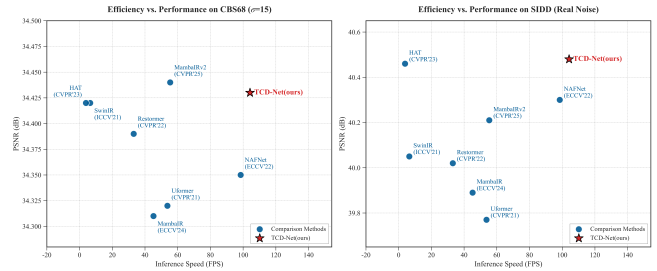


Figure 1: **Efficiency–performance trade-off.** PSNR vs. FPS on CBS68 ($\sigma=15$) and SIDD. TCD-Net achieves the best speed-quality trade-off among competing methods.

fine textures and noise often appear as high-frequency signals. Consequently, data-driven denoisers may exploit spurious correlations between environment factors and noise patterns and may fail to reliably separate subtle textures from random noise, leading to over-smoothing or residual artifacts.

Classical denoisers mitigate ill-posedness with hand-crafted priors such as BM3D [Dabov *et al.*, 2007], while learning-based methods learn data-driven mappings (e.g., DnCNN [Zhang *et al.*, 2017] and lightweight NAFNet [Chen *et al.*, 2022a]). For real photographs, complex camera/ISP noise motivates evaluation on SIDD/DND [Abdelhamed *et al.*, 2018; Plötz and Roth, 2017] and noise-aware modeling (e.g., DCBDNet) [Wu *et al.*, 2025]. Self/zero-shot schemes such as Noise2Void and Deep Image Prior further reduce reliance on clean targets [Krull *et al.*, 2019; Ulyanov *et al.*, 2018]. However, without explicit constraints on the generation process, many denoisers still entangle textures with stochastic noise via correlation-based fitting.

Transformers are increasingly adopted for image restoration. ViT demonstrates that global self-attention over patch tokens can be effective [Dosovitskiy *et al.*, 2021]. Hierarchical designs such as Swin Transformer enable scalable dense prediction [Liu *et al.*, 2021], and sophisticated restoration backbones, exemplified by Restormer and HAT, have demonstrated exceptional efficacy across denoising and related tasks [Zamir *et al.*, 2022; Chen *et al.*, 2023]. Yet, without explicit structural constraints, even strong backbones may learn shortcuts tied to nuisance cues and degrade under distribution changes.

Beyond attention, state-space models provide an efficient

alternative. Mamba introduces selective state spaces with linear-time sequence modeling [Gu and Dao, 2023], and recent restorers adapt this paradigm for image restoration, including MambaIR [Guo and others, 2024] and the UNet-like VMambaIR [Shi *et al.*, 2024]. Despite favorable efficiency and global receptive fields, SSM-based restorers can be sensitive to 2D inductive biases (e.g., scan/flatten order) and may aggregate local details less effectively than carefully designed attention or convolution modules, especially under real-noise and domain-shift settings.

In this work, we revisit denoising from a causal intervention perspective. Causal inference distinguishes correlation from causation by modeling data generation via structural causal models (SCMs) and reasoning about interventions [Pearl, 2009]. For denoising, the noisy observation arises from intrinsic content factors and extrinsic noise/environment factors; purely correlational fitting can therefore mix texture cues with nuisance variations in a single representation, harming robustness. Causal representation learning further argues that disentangling underlying causal factors is key to generalization and transfer [Schölkopf *et al.*, 2021]. This underscores the necessity of developing denoisers as structured interventions that suppress environment-induced bias, enforce factor separation, and improve identifiability.

Based on this causal formulation, we propose **TCD-Net** (Teacher-Guided Causal Disentanglement Network), a Vision Transformer denoiser that performs structured interventions to explicitly disentangle content and noise. We design an **Environmental Bias Adjustment (EBA)** module, a projection-and-restoration operator that removes token-wise bias and reinjects corrected features, to deconfound global environment shifts. We further design a **dual-head disentanglement** architecture to jointly predict the restored image and an explicit noise map, and enforce an **orthogonality constraint** between content/noise subspaces with **strong noise supervision** to prevent cross-branch leakage and anchor the noise branch. Finally, we incorporate a **teacher-guided causal prior** based on **Google Nano Banana Pro (NBP)** [Google DeepMind, 2025], which provides strong *zero-shot* restoration guidance and more natural high-frequency details [Zuo *et al.*, 2025]. To avoid over-trusting potentially hallucinated textures, we distill NBP only during training via a *feature-level* perceptual regularizer (instead of strict pixel matching), complementing perceptual supervision [Hinton *et al.*, 2015; Johnson *et al.*, 2016]. Moreover, since ViT-style absolute positional embeddings may break translation equivariance and rely on interpolation under resolution changes, we adopt resolution-adaptive conditional positional encoding (CPE) [Chu *et al.*, 2023] to mitigate positional representation shifts and improve robustness under distribution shifts.

Contributions. (1) We introduce a causal-intervention formulation for image denoising and instantiate it as TCD-Net, explicitly disentangling content and noise within a Vision Transformer. (2) We propose Environmental Bias Adjustment (EBA)-based deconfounding and orthogonal content–noise subspace constraints with strong noise supervision for anchoring. (3) We integrate a Google Nano Banana Pro (NBP)-guided causal prior to improve identifiability and perceptual

fidelity. (4) Extensive experiments and systematic ablations validate the effectiveness and efficiency of each component.

2 Related Work

2.1 Denoising Backbones: CNN/Transformer/SSM

Image denoising has progressed from hand-crafted priors such as BM3D [Dabov *et al.*, 2007] to learning-based mappings exemplified by residual CNNs (DnCNN) [Zhang *et al.*, 2017] and efficient modern designs (NAFNet) [Chen *et al.*, 2022a], while real camera noise benchmarks (SIDD/DND) expose the synthetic-to-real gap [Abdelhamed *et al.*, 2018; Plötz and Roth, 2017]. Recent restorers increasingly rely on global context modeling, including Transformer-based architectures (Restormer, HAT) [Zamir *et al.*, 2022; Chen *et al.*, 2023] and resolution-stable conditional positional encoding (CPE) [Chu *et al.*, 2023]. Beyond attention, state-space models provide linear-time global mixing via Mamba [Gu and Dao, 2023] and restoration adaptations such as MambaIR and VMambaIR [Guo and others, 2024; Shi *et al.*, 2024]. Despite these advances, stronger backbones or conditioning alone do not resolve the core ambiguity: without explicit structural constraints, models may still entangle textures with stochastic noise and overfit nuisance cues, degrading robustness under distribution shifts.

2.2 Generative/Teacher Priors and Causal Deconfounding

Generative priors—especially diffusion models—have been incorporated into restoration to enhance perceptual realism, including DiffIR [Xia *et al.*, 2023], DiffPIR [Zhu *et al.*, 2023], and DiffBIR [Lin *et al.*, 2024], which can recover visually pleasing textures but often require iterative sampling and may be sensitive to mismatched noise processes or prompts, raising deployment cost and stability concerns. From a causal viewpoint, denoising can be framed with SCMs and interventions [Pearl, 2009], where a key direction is to remove environment-induced confounders and separate content from nuisance noise for improved OOD robustness. In parallel, teacher guidance injects semantic priors via distillation [Hinton *et al.*, 2015]; we instantiate this idea with a *Google Nano Banana Pro* (NBP)-guided prior [Zuo *et al.*, 2025], which can be distilled once during training and keeps test-time inference single-pass, better fitting real-time denoising. To avoid over-trusting potentially hallucinated details, we distill NBP at the feature level and combine it with explicit factorization (a noise-map branch) and orthogonal subspace constraints, yielding a causal-factorized and efficient denoiser rather than a sampling-based generator.

3 Method

We instantiate the causal-intervention view in Introduction as a concrete Vision Transformer denoiser, **TCD-Net**, whose core goal is to *explicitly separate intrinsic content from extrinsic noise* and to *stabilize* this separation under environment/resolution shifts.

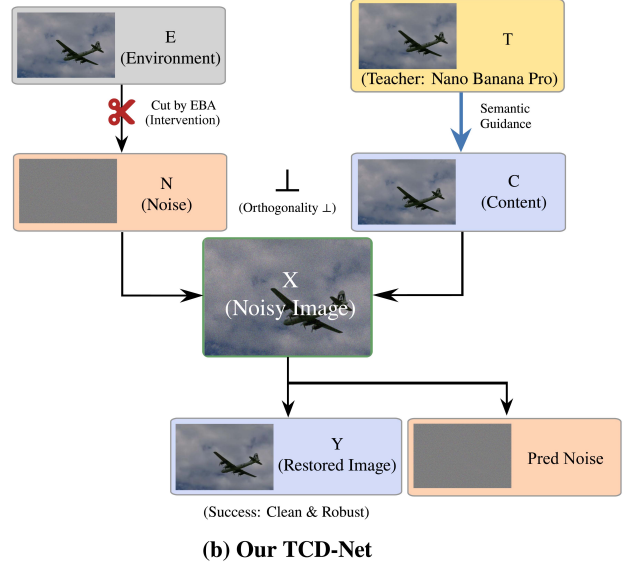
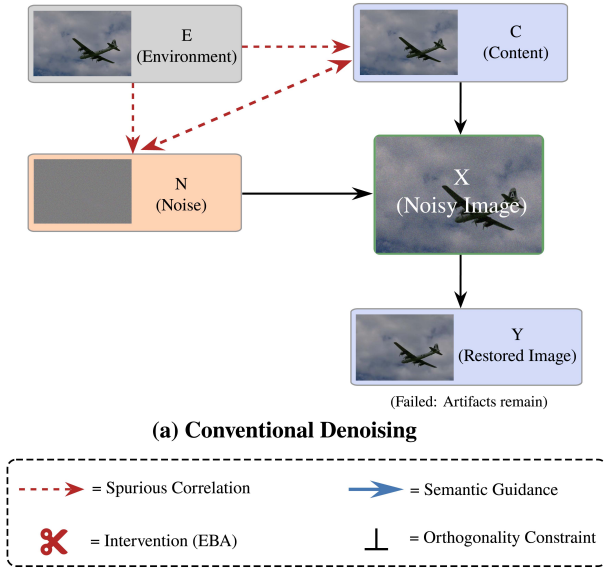


Figure 2: **Conceptual comparison between conventional denoising and TCD-Net.** (a) **Conventional denoising** is prone to spurious content–noise correlations induced by environmental factors E , leaving residual artifacts. (b) **TCD-Net** performs causal intervention via *EBA*, incorporates *teacher semantic guidance*, and enforces an *orthogonality constraint* to decouple content and noise for cleaner restoration.

3.1 Causal View and Overall Architecture

Let $Y \in \mathbb{R}^{H \times W \times 3}$ be the observed noisy image. We model Y as jointly generated by intrinsic **content** C (scene structures/textures) and extrinsic **noise** N (sensor/ISP corruption), under an **environment** factor E (illumination, gain, pipeline) that induces domain shift. A generic structural causal model (SCM) can be written as

$$\begin{aligned} C &:= f_C(U_C), & E &:= f_E(U_E), \\ N &:= f_N(C, E, U_N), & Y &:= f_Y(C, N, E), \end{aligned} \quad (1)$$

where U are exogenous variables. In denoising, we observe Y but must infer C . Given (1), learning content C from the observation Y by correlational fitting can spuriously couple C and noise N , especially in high-frequency regions where textures and noise overlap. We therefore design TCD-Net as structured interventions: EBA removes E -induced bias, a dual-branch head factorizes content/noise, an orthogonality constraint cuts leakage, explicit noise supervision anchors N , and an NBP-guided prior regularizes the content manifold.

Given an input Y , TCD-Net predicts both a restored image \hat{X} and an explicit noise map \hat{N} :

$$(\hat{X}, \hat{N}) = \mathcal{F}_\theta(Y). \quad (2)$$

The architecture is a JiT-style ViT denoiser that directly predicts clean content (on-manifold) while simultaneously modeling noise (off-manifold). Concretely, a Transformer encoder extracts mixed features Z_{all} , then a dual-branch head disentangles them into content features Z_c and noise features Z_n , which are decoded into \hat{X} and \hat{N} , respectively. The five causal interventions are implemented as: EBA-based de-confounding, dual-branch factorization, orthogonal subspace constraints, strong noise anchoring, and NBP-guided causal priors.

Fig. 2 illustrates why purely correlational denoising entangles content with noise, and how our causal intervention design explicitly breaks such spurious paths. The overall pipeline of TCD-Net is summarized in Fig. 3.

3.2 Transformer Backbone with Resolution-Stable Positional Encoding

We follow a ViT patch-tokenization pipeline. Given $Y \in \mathbb{R}^{H \times W \times 3}$, a convolutional patch embedding with patch size p produces a token grid:

$$T = \text{PatchEmbed}(Y) \in \mathbb{R}^{N \times d}, \quad N = \frac{H}{p} \cdot \frac{W}{p}. \quad (3)$$

We use a class token only for compatibility with standard ViT implementations and discard it for dense prediction. To mitigate positional representation shift under resolution changes (noted in Introduction), we use a hybrid positional scheme: (i) interpolated absolute embeddings, where the embedding grid is bicubically interpolated to match $(H/p, W/p)$ when needed; and (ii) conditional positional encoding (CPE), where each block injects a depth-wise 3×3 convolutional positional signal computed from the *current* token features. Let $T^{(\ell)}$ be tokens at block ℓ reshaped to a feature map $\mathcal{R}(T^{(\ell)}) \in \mathbb{R}^{d \times H/p \times W/p}$. Then

$$T^{(\ell)} \leftarrow T^{(\ell)} + \text{Flatten}\left(\text{DWConv}_{3 \times 3}(\mathcal{R}(T^{(\ell)}))\right). \quad (4)$$

After CPE injection, each block applies MHSA and an MLP, yielding updated patch tokens. To further improve invariance to environment shifts, we append an EBA de-confounding module at the end of each block.

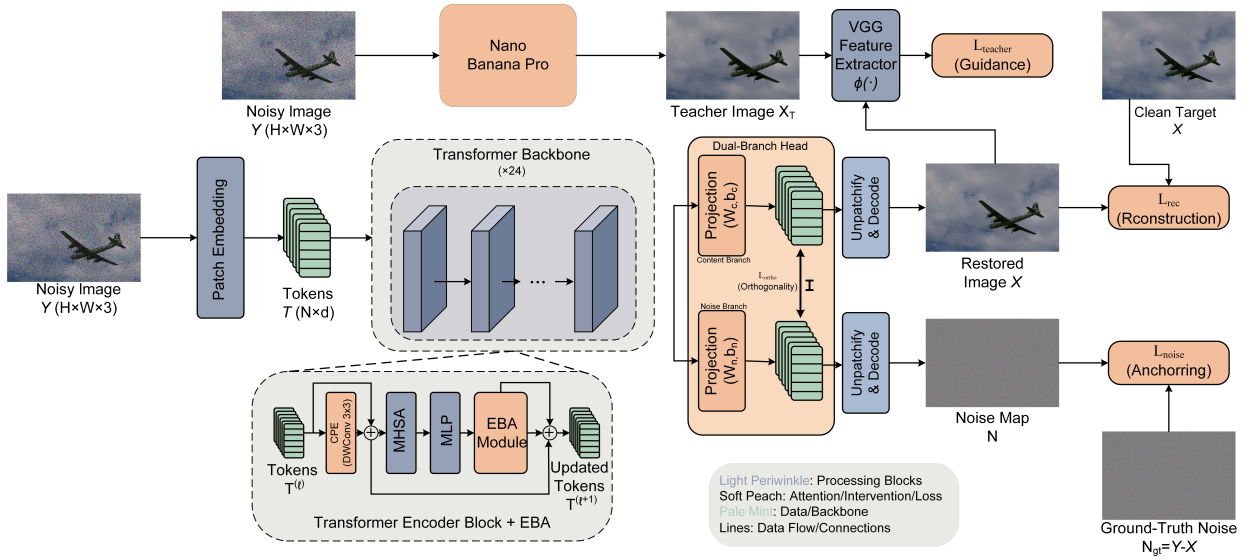


Figure 3: **Overview of TCD-Net.** A ViT backbone with EBA feeds a dual-branch head to predict the restored image \hat{X} and noise map \hat{N} , trained with orthogonality, noise anchoring, and teacher guidance.

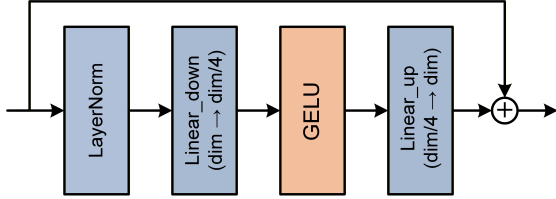


Figure 4: **EBA module.** LayerNorm + bottleneck MLP with residual projection to suppress environment-induced bias and stabilize token representations.

3.3 Causal Interventions: De-confounding, Disentanglement, and NBP Guidance

Environmental Bias Adjustment (EBA) de-confounding. Real noisy images often contain global appearance shifts (e.g., illumination/color temperature) that act as environment-induced confounders E . We implement de-confounding with our **Environmental Bias Adjustment (EBA)** module and is embedded at the end of each Transformer block. For a token feature $t \in \mathbb{R}^d$, EBA performs (i) **explicit de-centering**, (ii) **projection** via a bottleneck MLP, and (iii) **affine restoration** via a residual connection:

$$\mu(t) = \frac{1}{d} \mathbf{1}^\top t, \quad \tilde{t} = t - \mu(t) \mathbf{1}, \quad (5)$$

$$\text{EBA}(t) = t + W_2 \sigma(W_1 \text{LN}(\tilde{t})), \quad (6)$$

where $\text{LN}(\cdot)$ is LayerNorm, $\sigma(\cdot)$ is GELU, and W_1, W_2 are learnable projections. Intuitively, removing the per-token centroid suppresses global bias components, while the learnable projection pushes features toward a more stable subspace before being added back. The concrete operator structure of EBA is shown in Fig. 4.

Dual-branch content–noise disentanglement and orthogonality. Let $Z_{\text{all}} \in \mathbb{R}^{N \times d}$ denote the final encoder patch-

token features. We explicitly parameterize two branches:

$$Z_c = Z_{\text{all}} W_c + b_c, \quad Z_n = Z_{\text{all}} W_n + b_n, \quad (7)$$

where (W_c, b_c) and (W_n, b_n) are learned linear projections. Each branch predicts patch-wise RGB values, then we *unpatchify* to the image plane:

$$\hat{X} = \text{Unpatchify}(Z_c W_x + b_x), \quad (8)$$

$$\hat{N} = \text{Unpatchify}(Z_n W'_n + b'_n), \quad (9)$$

where Unpatchify reshapes patch predictions back to full resolution. To prevent cross-branch leakage (textures encoded as “noise” or noise contaminating content), we impose an orthogonality constraint between token-wise content/noise subspaces:

$$\mathcal{L}_{\text{ortho}} = \frac{1}{BN} \sum_{b=1}^B \sum_{i=1}^N \left\langle \frac{z_c^{(b,i)}}{\|z_c^{(b,i)}\|_2}, \frac{z_n^{(b,i)}}{\|z_n^{(b,i)}\|_2} \right\rangle. \quad (10)$$

Minimizing (10) acts as a geometric firewall: content-like directions are discouraged from entering the noise channel. A pure orthogonality regularizer can admit degenerate solutions (e.g., collapsing Z_n), so we additionally *anchor* the nuisance mechanism with explicit noise supervision. For paired training with known clean target X , the ground-truth noise is

$$N_{\text{gt}} = Y - X. \quad (11)$$

Teacher-guided causal prior. Denoising is ill-posed: multiple clean images can explain the same noisy observation. To improve identifiability and perceptual fidelity, we leverage a **Google Nano Banana Pro (NBP)-guided causal prior**. During training, for some samples we obtain an auxiliary teacher image X^T by applying NBP in an image-to-image editing setting with a denoising/clean-up prompt. Prior evaluations suggest that NBP often produces high-quality, visually pleasing restorations (especially high-frequency details) in a

zero-shot manner [Zuo *et al.*, 2025]. Since NBP outputs may contain plausible but input-inconsistent details, we adopt X^T as a *perceptual* target and enforce feature alignment with a fixed VGG extractor $\phi(\cdot)$:

$$\mathcal{L}_{\text{teacher}} = \|\phi(\hat{X}) - \phi(X^T)\|_1. \quad (12)$$

This distills semantic/texture priors from NBP [Hinton *et al.*, 2015], pulling \hat{X} toward the natural- image manifold while remaining faithful to the input content. In implementation, we apply identical random crop/flip/rotation to (X, X^T) to avoid misalignment.

3.4 Optimization and Inference

We use the Charbonnier penalty (a robust L_1 surrogate) $\rho(a) = \sqrt{a^2 + \epsilon^2}$ for pixel-level supervision. The overall objective is

$$\mathcal{L} = \mathcal{L}_{\text{rec}} + \lambda_{\text{noise}}\mathcal{L}_{\text{noise}} + \lambda_{\text{ortho}}\mathcal{L}_{\text{ortho}} + \lambda_{\text{teacher}}\mathcal{L}_{\text{teacher}}, \quad (13a)$$

$$\mathcal{L}_{\text{rec}} = \frac{1}{|\Omega|} \sum_{u \in \Omega} \rho(\hat{X}(u) - X(u)), \quad (13b)$$

$$\mathcal{L}_{\text{noise}} = \frac{1}{|\Omega|} \sum_{u \in \Omega} \rho(\hat{N}(u) - N_{\text{gt}}(u)), \quad (13c)$$

where $\lambda_{\text{noise}}, \lambda_{\text{ortho}}, \lambda_{\text{teacher}}$ balance the interventions. When X^T is unavailable, we set $\mathcal{L}_{\text{teacher}} = 0$.

Thanks to patch tokenization and dynamic positional interpolation, TCD-Net supports variable resolutions. For high-resolution images where full attention becomes memory-intensive, we adopt an overlap-tile inference with Gaussian blending. We split Y into overlapping patches $\{Y_k\}$ (patch size P , stride $S < P$), predict $\hat{X}_k = \mathcal{F}_\theta(Y_k)$, and blend them via a Gaussian weight map W whose standard deviation is set to $P/4$:

$$\hat{X} = \frac{\sum_k W \odot \hat{X}_k}{\sum_k W + \epsilon}. \quad (14)$$

This reduces blocking artifacts at tile boundaries and stabilizes performance under resolution changes.

4 Experiments

4.1 Experimental Setup

Tasks and benchmarks. We evaluate TCD-Net on (i) *synthetic* color Gaussian denoising and (ii) *real-world* denoising. For synthetic denoising, we follow the standard blind AWGN protocol [Zhang *et al.*, 2017; Zhang *et al.*, 2018a]: during training, σ is uniformly sampled from $[0, 50]$ and added to clean RGB patches; during testing, we report PSNR (dB) at $\sigma \in \{15, 25, 50\}$ on CBSD68 [Arbelaz *et al.*, 2011; Zhang *et al.*, 2017], Kodak24 [Franzen, 1999], McMaster [Zhang *et al.*, 2011], and Urban100 [Huang *et al.*, 2015]. For real-world denoising, we report PSNR/SSIM [Wang *et al.*, 2004] on SIDD [Abdelhamed *et al.*, 2018] and DND [Plotz and Roth, 2017], and additionally report LPIPS [Zhang *et al.*, 2018b] (lower is better) on SIDD and on Urban100 at $\sigma=50$. All real-noise results are obtained by *fine-tuning* a synthetic-pretrained model: we start from a DF2K-trained Gaussian

denoiser (DIV2K+Flicker2K) [Agustsson and Timofte, 2017; Lim *et al.*, 2017] and fine-tune on SIDD and DND following their training protocols.

Implementation and training. Unless specified otherwise, we use a ViT-L/16 backbone [Dosovitskiy *et al.*, 2021] (dim 1024, depth 24, 16 heads) with the causal interventions in Section 3. We train on DF2K [Agustsson and Timofte, 2017; Lim *et al.*, 2017] using random 256×256 crops and synchronized augmentations (crop/flip/rotation) for (Y, X) and teacher images, and optimize with AdamW [Loshchilov and Hutter, 2019] using cosine learning-rate decay [Loshchilov and Hutter, 2017] and weight decay $1e-4$. We adopt a two-stage schedule: *Stage 1* trains for 100 epochs (lr $2e-4$, batch 32, repetition 20) with reconstruction, noise supervision, and orthogonality ($\lambda_{\text{noise}}=0.5$, $\lambda_{\text{ortho}}=0.1$); *Stage 2* fine-tunes for 50 epochs (lr $5e-5$) enabling teacher guidance (weight 0.1) and slightly reducing regularization ($\lambda_{\text{noise}}=0.25$, $\lambda_{\text{ortho}}=0.05$). For **real-world** denoising, we initialize from the DF2K-trained model and **fine-tune on SIDD/DND** with the same objectives (Eq. (13)), disabling synthetic noise injection and using dataset-provided noisy/clean pairs for supervision [Abdelhamed *et al.*, 2018; Plotz and Roth, 2017].

Hardware and software. All experiments are implemented in PyTorch 2.8.0 with Python 3.12 on Ubuntu 22.04, using CUDA 12.8. For runtime measurements (FPS/latency), we use a single RTX 5090 (32GB), 25 vCPU Intel(R) Xeon(R) Platinum 8470Q, and 90GB RAM. Latency is measured with batch size 1 at resolution 256×256 after warm-up, and FPS is computed as the reciprocal of mean latency.

Baselines. We compare with a classical prior (BM3D [Dabov *et al.*, 2007]), representative CNN denoisers (DnCNN [Zhang *et al.*, 2017], CBDNet [Guo *et al.*, 2019], RIDNet [Anwar and Barnes, 2019], DRUNet [Zhang *et al.*, 2021]), and modern Transformer/state-space restorers (SwinIR [Liang *et al.*, 2021], DAGL [Mou *et al.*, 2021], MPRNet [Zamir *et al.*, 2021], SCUNet [Zhang *et al.*, 2023], Uformer [Wang *et al.*, 2022], Restormer [Zamir *et al.*, 2022], NAFNet [Chen *et al.*, 2022b], HAT [Chen *et al.*, 2023], MambaIR [Guo and others, 2024], MambaIRv2 [Guo *et al.*, 2025]). We follow standard benchmark protocols and report results from official implementations or widely adopted reported numbers.

4.2 Results on Synthetic Gaussian Denoising

Table 1 reports PSNR/SSIM comparisons of TCD-Net against recent CNN/Transformer/SSM-based restorers on four benchmarks. Overall, TCD-Net achieves *consistently strong* performance and excels on texture-rich datasets, obtaining the **best** PSNR on McMaster for all $\sigma \in \{15, 25, 50\}$ and on Urban100 at $\sigma=25/50$ (runner-up at $\sigma=15$), while remaining top-tier on CBSD68 across noise levels. The gains under heavy noise (e.g., $\sigma=50$) align with our causal design: explicit noise supervision provides an identifiable nuisance handle, and the orthogonality constraint reduces content-noise cross-talk that causes over-smoothing or residual noise-like details. Moreover, CPE alleviates resolution-induced representation shifts and EBA mitigates environment-related

Method	Venue	CBSD68			Kodak24			McMaster			Urban100		
		$\sigma=15$	$\sigma=25$	$\sigma=50$									
DnCNN	TIP'17	33.90	31.24	27.95	34.60	32.14	28.95	33.45	31.52	28.62	32.98	30.81	27.59
DRUNet	TPAMI'21	34.30	31.69	28.51	35.31	32.89	29.86	35.40	33.14	30.08	34.81	32.60	29.61
SwinIR	ICCV'21	34.42	31.78	28.56	35.34	32.89	29.79	35.61	33.20	30.22	35.13	32.90	29.82
SCUNet	AAAI'22	34.40	<u>31.79</u>	28.61	35.34	32.92	29.87	35.60	<u>33.34</u>	<u>30.29</u>	35.18	33.03	30.14
Restormer	CVPR'22	34.39	31.78	28.59	<u>35.44</u>	33.02	30.00	35.55	33.31	<u>30.29</u>	35.06	32.91	30.02
NAFNet	ECCV'22	—	—	28.39	—	—	29.64	—	—	29.98	—	—	29.71
HAT	CVPR'23	34.42	<u>31.79</u>	28.58	35.46	<u>33.03</u>	<u>30.01</u>	<u>35.62</u>	<u>33.34</u>	30.26	35.37	<u>33.14</u>	<u>30.23</u>
MambaIR	ECCV'24	34.31	<u>31.66</u>	28.47	35.33	32.82	29.94	35.40	33.15	30.06	35.17	32.99	30.07
MambaIRv2	CVPR'25	34.44	31.78	28.66	<u>35.44</u>	33.05	30.02	35.55	33.31	30.28	35.27	<u>33.14</u>	30.21
TCD-Net	—	<u>34.43</u>	31.80	<u>28.64</u>	35.43	32.99	30.00	35.64	33.35	30.34	<u>35.35</u>	33.16	30.27

Table 1: Color Gaussian denoising results (PSNR, dB) on standard benchmarks at $\sigma \in \{15, 25, 50\}$. Best and second best are highlighted.

Dataset	Metric	BM3D TIP'07	DnCNN TIP'17	CBDDNet CVPR'19	RIDNet ICCV'19	MPRNet CVPR'21	DAGL ICCV'21	SwinIR ICCV'21	Uformer CVPR'22	Restormer CVPR'22	NAFNet ECCV'22	HAT CVPR'23	MambaIR ECCV'24	MambaIRv2 CVPR'25	TCD-Net (ours)
SIDD	PSNR	25.65	23.66	30.78	38.71	39.71	38.94	40.05	39.77	40.02	40.30	<u>40.46</u>	39.89	40.21	40.48
	SSIM	0.685	0.583	0.801	0.951	0.958	0.953	0.961	0.959	0.960	0.962	<u>0.964</u>	0.960	0.963	0.965
DND	PSNR	34.51	32.43	38.06	39.26	39.80	39.77	39.91	39.96	40.03	40.27	<u>40.44</u>	—	—	40.45
	SSIM	0.851	0.790	0.942	0.953	0.954	0.956	0.961	0.956	0.956	0.957	0.958	—	—	<u>0.960</u>

Table 2: **Real-world denoising** on SIDD and DND (PSNR/SSIM). We fine-tune the DF2K pretrained model on SIDD and DND, respectively. Best and second best are highlighted.

Method	Venue	SIDD	Urban100 ($\sigma=50$)
SwinIR	ICCV'21	0.142	0.210
Uformer	CVPR'22	0.140	0.205
Restormer	CVPR'22	0.138	0.198
NAFNet	ECCV'22	0.135	0.195
HAT	CVPR'23	0.131	0.188
MambaIR	ECCV'24	0.125	0.182
MambaIRv2	CVPR'25	0.118	0.174
TCD-Net	—	0.128	0.184

Table 3: Perceptual quality comparison using LPIPS (lower is better) on SIDD and Urban100 ($\sigma=50$).

Method	Venue	FLOPs (G)	Time (ms)	FPS	Gaussian PSNR	Real-world PSNR
SwinIR	ICCV'21	804.7	154.47	6.5	34.42	40.05
Uformer	CVPR'22	86.9	18.63	53.7	34.32	39.77
Restormer	CVPR'22	154.9	30.22	33.1	34.39	40.02
NAFNet	ECCV'22	16.3	<u>10.15</u>	<u>98.5</u>	34.35	40.30
HAT	CVPR'23	721.3	258.75	3.9	34.42	<u>40.46</u>
MambaIR	ECCV'24	<u>68.2</u>	22.12	45.2	34.31	39.89
MambaIRv2	CVPR'25	69.5	18.05	55.4	34.44	40.21
TCD-Net	—	84.8	9.59	104.2	<u>34.43</u>	40.48

Table 4: Efficiency comparison. FLOPs are reported for a single forward pass. Latency/FPS are measured at 256×256 with batch size 1. Best and second best are highlighted.

bias, improving stability across settings. Together with Table 4, TCD-Net provides a practical quality–speed trade-off by emphasizing robustness via explicit mechanism separation rather than backbone scaling.

ID	Dual-Stream & $\mathcal{L}_{\text{noise}}$	$\mathcal{L}_{\text{ortho}}$ (Indep.)	Pos. Enc.	EBA Topology	$\mathcal{L}_{\text{teacher}}$ (Prior)	PSNR
1	×	×	APE	×	×	31.35
2	✓	×	APE	×	×	31.36
3	✓	✓	CPE	×	×	31.48
4	✓	✓	CPE	Parallel	×	31.60
5	✓	✓	CPE	Serial	×	31.77
6	✓	✓	CPE	Serial	✓	31.80

Table 5: Ablation on CBSD68 validation at $\sigma=25$ (PSNR, dB). We incrementally add the dual-stream design with noise supervision, the independent orthogonality regularizer, CPE, the EBA module, and the teacher prior. Best and second best are highlighted.

4.3 Real-World Adaptation, Efficiency, and Ablations

Real-world results: fine-tuning from the Gaussian model. Table 2 reports performance on real noisy photographs. Starting from the DF2K-trained Gaussian model and fine-tuning on SIDD/DND, TCD-Net achieves the **best** PSNR/SSIM on SIDD and the **best** PSNR on DND, indicating strong synthetic-to-real transfer. Notably, it also attains competitive DND SSIM (runner-up), suggesting that the explicit nuisance branch and the de-confounding components help adapt to signal-dependent noise and camera pipeline variations during fine-tuning.

Perceptual quality: LPIPS. Besides distortion metrics, we report LPIPS [Zhang *et al.*, 2018b] on SIDD and Urban100 ($\sigma=50$) to better reflect perceptual similarity. Table 3 reports LPIPS (lower is better) for perceptual comparison. TCD-

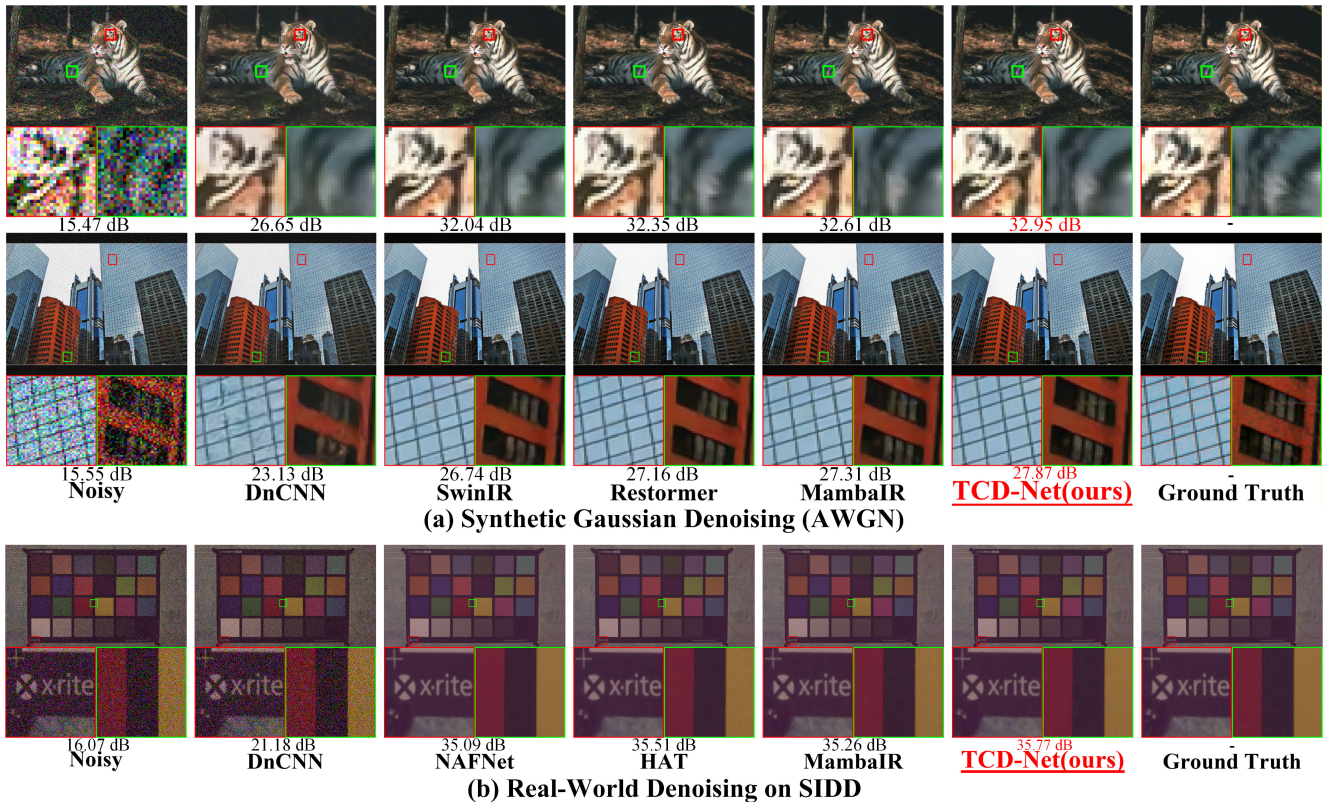


Figure 5: **Qualitative comparison on synthetic and real noise.** (a) **Synthetic Gaussian denoising (AWGN).** (b) **Real-world denoising on SIDD.** Conventional methods may leave residual noise or oversmooth details due to spurious content–noise correlation. With EBA-based intervention, orthogonal disentanglement, and teacher guidance, TCD-Net restores cleaner results with sharper textures and edges.

Net achieves competitive perceptual quality (e.g., 0.128 on SIDD and 0.184 on Urban100 at $\sigma=50$), outperforming several strong Transformer baselines, while the best LPIPS is obtained by the latest SSM-based restorers. This suggests that our explicit content–noise separation preserves perceptual fidelity, though there remains room to further improve perceptual alignment.

Efficiency: fast inference with a simple, single-path Transformer. Beyond restoration fidelity, we emphasize that TCD-Net is designed to be efficient at inference. As shown in Table 4, TCD-Net achieves the **lowest latency** (9.59 ms) and the **highest FPS** (104.2) among all compared methods on our hardware, while maintaining strong denoising quality. Although its FLOPs are not the smallest, the computation graph is intentionally simple and straightforward (patch embedding \rightarrow stacked Transformer blocks \rightarrow lightweight dual heads), which favors GPU parallelism and reduces synchronization overhead in practice.

Ablation: effects of causal components and teacher prior. Table 5 shows that the proposed modules contribute *complementarily*. A naive dual-head yields only a marginal gain (ID 1 \rightarrow 2, +0.01 dB), indicating that architectural splitting alone does not guarantee disentanglement. Adding the orthogonality regularizer and switching to CPE brings a larger improvement (ID 2 \rightarrow 3, +0.12 dB), suggesting reduced content–noise leakage and more stable dense prediction un-

der positional shifts. Introducing EBA further boosts PSNR (ID 3 \rightarrow 4/5), and the serial topology outperforms the parallel one (ID 4 \rightarrow 5, +0.17 dB). Finally, enabling the NBP teacher prior provides an additional gain (ID 5 \rightarrow 6, +0.03 dB), consistent with improved identifiability by pulling the content prediction toward the natural-image manifold; this teacher loss is applied only during training and incurs no inference cost.

5 Conclusion

We revisit image denoising from a causal-intervention perspective, where correlation-based fitting can entangle intrinsic content with extrinsic noise, degrading robustness under high-frequency ambiguity and distribution shifts. We propose TCD-Net, a Vision Transformer denoiser with structured interventions for content–noise disentanglement: EBA deconfounds environment bias via de-centered projection with residual restoration, and a dual-branch head with orthogonality plus strong noise supervision reduces leakage and anchors the nuisance factor. We further distill an NBP-guided feature-level perceptual prior to regularize content toward the natural-image manifold, and adopt resolution-stable positional encoding for better generalization. Experiments on synthetic Gaussian and real benchmarks show state-of-the-art or competitive fidelity with high efficiency (9.59 ms, 104.2 FPS on RTX 5090). Future work will explore reliability-aware teacher priors and causal intervention learning under domain shift and weak supervision for real-world noise.

References

- [Abdelhamed *et al.*, 2018] Abdelrahman Abdelhamed, Stephen Lin, and Michael S. Brown. A high-quality denoising dataset for smartphone cameras. In *Proceedings of the IEEE Conference on Computer Vision and Pattern Recognition (CVPR)*, pages 1692–1700, 2018.
- [Agustsson and Timofte, 2017] Eirikur Agustsson and Radu Timofte. NTIRE 2017 challenge on single image super-resolution: Dataset and study. In *Proceedings of the IEEE Conference on Computer Vision and Pattern Recognition (CVPR) Workshops*, 2017.
- [Anwar and Barnes, 2019] Saeed Anwar and Nick Barnes. Real image denoising with feature attention. In *Proceedings of the IEEE/CVF International Conference on Computer Vision (ICCV)*, pages 3155–3164, 2019.
- [Arbeláez *et al.*, 2011] Pablo Arbeláez, Michael Maire, Charless Fowlkes, and Jitendra Malik. Contour detection and hierarchical image segmentation. *IEEE Transactions on Pattern Analysis and Machine Intelligence*, 33(5):898–916, 2011.
- [Chen *et al.*, 2022a] Liangyu Chen, Xiaojie Chu, Xiangyu Zhang, and Jian Sun. Simple baselines for image restoration. In *European Conference on Computer Vision (ECCV)*, 2022.
- [Chen *et al.*, 2022b] Liangyu Chen, Xiaojie Chu, Xiangyu Zhang, and Jian Sun. Simple baselines for image restoration. In *Computer Vision – ECCV 2022*, pages 17–33, 2022.
- [Chen *et al.*, 2023] Xiangyu Chen, Xintao Wang, Wenlong Zhang, Xiangtao Kong, Yu Qiao, Jiantao Zhou, and Chao Dong. Hat: Hybrid attention transformer for image restoration. *arXiv preprint arXiv:2309.05239*, 2023.
- [Chu *et al.*, 2023] Xiaojie Chu, Zhi Tian, Yuqing Wang, Bo Zhang, Haibing Ren, Xiaolin Wei, Huaxia Xia, and Chunhua Shen. Conditional positional encodings for vision transformers. In *International Conference on Learning Representations (ICLR)*, 2023.
- [Dabov *et al.*, 2007] Kostadin Dabov, Alessandro Foi, Vladimir Katkovnik, and Karen Egiazarian. Image denoising by sparse 3-d transform-domain collaborative filtering. *IEEE Transactions on Image Processing*, 16(8):2080–2095, 2007.
- [Dosovitskiy *et al.*, 2021] Alexey Dosovitskiy, Lucas Beyer, Alexander Kolesnikov, Dirk Weissenborn, Xiaohua Zhai, Thomas Unterthiner, Mostafa Dehghani, Matthias Minderer, Georg Heigold, Sylvain Gelly, Jakob Uszkoreit, and Neil Houlsby. An image is worth 16x16 words: Transformers for image recognition at scale. In *International Conference on Learning Representations (ICLR)*, 2021.
- [Franzen, 1999] Rich Franzen. Kodak lossless true color image suite. <http://r0k.us/graphics/kodak/>, 1999. Accessed: 2026-01-10.
- [Google DeepMind, 2025] Google DeepMind. Introducing nano banana pro. <https://blog.google/innovation-and-ai/products/nano-banana-pro/>, November 2025.
- [Gu and Dao, 2023] Albert Gu and Tri Dao. Mamba: Linear-time sequence modeling with selective state spaces. *arXiv preprint arXiv:2312.00752*, 2023.
- [Guo and others, 2024] Hang Guo et al. Mambair: A simple baseline for image restoration with state-space model. *arXiv preprint arXiv:2402.15648*, 2024. Accepted by ECCV 2024.
- [Guo *et al.*, 2019] Shi Guo, Zifei Yan, Kai Zhang, Wang-meng Zuo, and Lei Zhang. Toward convolutional blind denoising of real photographs. In *Proceedings of the IEEE/CVF Conference on Computer Vision and Pattern Recognition (CVPR)*, pages 1712–1722, 2019.
- [Guo *et al.*, 2025] Hang Guo, Yong Guo, Yaohua Zha, Yulun Zhang, Wenbo Li, Tao Dai, Shu-Tao Xia, and Yawei Li. Mambairv2: Attentive state space restoration. In *Proceedings of the IEEE/CVF Conference on Computer Vision and Pattern Recognition (CVPR)*, pages 28124–28133, June 2025.
- [Hinton *et al.*, 2015] Geoffrey Hinton, Oriol Vinyals, and Jeffrey Dean. Distilling the knowledge in a neural network. *arXiv preprint arXiv:1503.02531*, 2015.
- [Huang *et al.*, 2015] Jia-Bin Huang, Abhishek Singh, and Narendra Ahuja. Single image super-resolution from transformed self-exemplars. In *Proceedings of the IEEE Conference on Computer Vision and Pattern Recognition (CVPR)*, pages 5197–5206, June 2015.
- [Johnson *et al.*, 2016] Justin Johnson, Alexandre Alahi, and Li Fei-Fei. Perceptual losses for real-time style transfer and super-resolution. In *Computer Vision – ECCV 2016*, pages 694–711, 2016.
- [Krull *et al.*, 2019] Alexander Krull, Tim-Oliver Buchholz, and Florian Jug. Noise2void: Learning denoising from single noisy images. In *Proceedings of the IEEE/CVF Conference on Computer Vision and Pattern Recognition (CVPR)*, pages 2129–2137, 2019.
- [Liang *et al.*, 2021] Jingyun Liang, Jiezhang Cao, Guo-Cheng Wang, Kai Zhang, Lei Zhang, Luc Van Gool, and Radu Timofte. SwinIR: Image restoration using swin transformer, 2021.
- [Lim *et al.*, 2017] Bee Lim, Sanghyun Son, Heewon Kim, Seungjun Nah, and Kyoung Mu Lee. Enhanced deep residual networks for single image super-resolution. In *Proceedings of the IEEE Conference on Computer Vision and Pattern Recognition (CVPR) Workshops*, pages 1132–1140, 2017.
- [Lin *et al.*, 2024] Xinqi Lin, Jingwen He, Ziyang Chen, Zhaoyang Lyu, Bo Dai, Fanghua Yu, Wanli Ouyang, Yu Qiao, and Chao Dong. Diffbir: Towards blind image restoration with generative diffusion prior. *arXiv preprint arXiv:2308.15070*, 2024.
- [Liu *et al.*, 2021] Ze Liu, Yutong Lin, Yue Cao, Han Hu, Yixuan Wei, Zheng Zhang, Stephen Lin, and Baining Guo. Swin transformer: Hierarchical vision transformer using shifted windows. In *Proceedings of the IEEE/CVF International Conference on Computer Vision (ICCV)*, pages 10012–10022, 2021.

- [Loshchilov and Hutter, 2017] Ilya Loshchilov and Frank Hutter. SGDR: Stochastic gradient descent with warm restarts. In *International Conference on Learning Representations (ICLR)*, 2017. arXiv:1608.03983.
- [Loshchilov and Hutter, 2019] Ilya Loshchilov and Frank Hutter. Decoupled weight decay regularization. In *International Conference on Learning Representations (ICLR)*, 2019. arXiv:1711.05101.
- [Mou et al., 2021] Chong Mou, Jian Zhang, and Zhuoyuan Wu. Dynamic attentive graph learning for image restoration. In *Proceedings of the IEEE/CVF International Conference on Computer Vision (ICCV)*, pages 4328–4337, October 2021.
- [Pearl, 2009] Judea Pearl. *Causality: Models, Reasoning, and Inference*. Cambridge University Press, 2 edition, 2009.
- [Plötz and Roth, 2017] Tobias Plötz and Stefan Roth. Benchmarking denoising algorithms with real photographs. In *Proceedings of the IEEE Conference on Computer Vision and Pattern Recognition (CVPR)*, pages 2750–2759, 2017.
- [Schölkopf et al., 2021] Bernhard Schölkopf, Francesco Locatello, Stefan Bauer, Nan Rosemary Ke, Nal Kalchbrenner, Anirudh Goyal, and Yoshua Bengio. Toward causal representation learning. *Proceedings of the IEEE*, 109(5):612–634, 2021.
- [Shi et al., 2024] Yuan Shi, Bin Xia, Xiaoyu Jin, Xing Wang, Tianyu Zhao, Xin Xia, Xuefeng Xiao, and Wenming Yang. Vmambair: Visual state space model for image restoration. *arXiv preprint arXiv:2403.11423*, 2024.
- [Ulyanov et al., 2018] Dmitry Ulyanov, Andrea Vedaldi, and Victor Lempitsky. Deep image prior. In *Proceedings of the IEEE Conference on Computer Vision and Pattern Recognition (CVPR)*, pages 9446–9454, 2018.
- [Wang et al., 2004] Zhou Wang, Alan C. Bovik, Hamid R. Sheikh, and Eero P. Simoncelli. Image quality assessment: From error visibility to structural similarity. *IEEE Transactions on Image Processing*, 13(4):600–612, 2004.
- [Wang et al., 2022] Zhendong Wang, Xiaodong Cun, Jianmin Bao, Wengang Zhou, Jianzhuang Liu, and Houqiang Li. Uformer: A general u-shaped transformer for image restoration. In *Proceedings of the IEEE/CVF Conference on Computer Vision and Pattern Recognition (CVPR)*, pages 17683–17693, 2022.
- [Wu et al., 2025] Wencong Wu, Shicheng Liao, Guannan Lv, Peng Liang, and Yungang Zhang. Image blind denoising using dual convolutional neural network with skip connection. *Signal Processing: Image Communication*, 138:117365, 2025.
- [Xia et al., 2023] Bin Xia, Yulun Zhang, Shiyin Wang, Yitong Wang, Xinglong Wu, Yapeng Tian, Wenming Yang, and Luc Van Gool. Diffir: Efficient diffusion model for image restoration. In *Proceedings of the IEEE/CVF International Conference on Computer Vision (ICCV)*, 2023.
- [Zamir et al., 2021] Syed Waqas Zamir, Aditya Arora, Salman Khan, Munawar Hayat, Fahad Shahbaz Khan, Ming-Hsuan Yang, and Ling Shao. Multi-stage progressive image restoration. In *Proceedings of the IEEE/CVF Conference on Computer Vision and Pattern Recognition (CVPR)*, pages 14821–14831, 2021.
- [Zamir et al., 2022] Syed Waqas Zamir, Aditya Arora, Salman Khan, Munawar Hayat, Fahad Shahbaz Khan, and Ming-Hsuan Yang. Restormer: Efficient transformer for high-resolution image restoration. In *Proceedings of the IEEE/CVF Conference on Computer Vision and Pattern Recognition (CVPR)*, pages 5728–5739, 2022.
- [Zhang et al., 2011] Lei Zhang, Xiaolin Wu, Antoni Buades, and Xin Li. Color demosaicking by local directional interpolation and nonlocal adaptive thresholding. *Journal of Electronic Imaging*, 20(2):023016, 2011.
- [Zhang et al., 2017] Kai Zhang, Wangmeng Zuo, Yunjin Chen, Deyu Meng, and Lei Zhang. Beyond a gaussian denoiser: Residual learning of deep CNN for image denoising. In *Proceedings of the IEEE Conference on Computer Vision and Pattern Recognition (CVPR)*, pages 3929–3937, 2017.
- [Zhang et al., 2018a] Kai Zhang, Wangmeng Zuo, and Lei Zhang. FFDNet: Toward a fast and flexible solution for CNN-based image denoising. *IEEE Transactions on Image Processing*, 27(9):4608–4622, 2018.
- [Zhang et al., 2018b] Richard Zhang, Phillip Isola, Alexei A. Efros, Eli Shechtman, and Oliver Wang. The unreasonable effectiveness of deep features as a perceptual metric. In *Proceedings of the IEEE/CVF Conference on Computer Vision and Pattern Recognition (CVPR)*, 2018.
- [Zhang et al., 2021] Kai Zhang, Yawei Li, Wangmeng Zuo, Lei Zhang, Luc Van Gool, and Radu Timofte. Plug-and-play image restoration with deep denoiser prior. *arXiv preprint arXiv:2008.13751*, 2021.
- [Zhang et al., 2023] Kai Zhang, Yawei Li, Jingyun Liang, Jie Zhang Cao, Yulun Zhang, Hao Tang, Deng-Ping Fan, Radu Timofte, and Luc Van Gool. Practical blind image denoising via swin-conv-UNet and data synthesis. *Machine Intelligence Research*, 2023.
- [Zhu et al., 2023] Yuanzhi Zhu, Kai Zhang, Jingyun Liang, Jie Zhang Cao, Bihan Wen, Radu Timofte, and Luc Van Gool. Denoising diffusion models for plug-and-play image restoration. *arXiv preprint arXiv:2305.08995*, 2023.
- [Zuo et al., 2025] Jialong Zuo, Haoyou Deng, Hanyu Zhou, Jiaxin Zhu, Yicheng Zhang, Yiwei Zhang, Yongxin Yan, Kaixing Huang, Weisen Chen, Yongtai Deng, Rui Jin, Nong Sang, and Changxin Gao. Is nano banana pro a low-level vision all-rounder? a comprehensive evaluation on 14 tasks and 40 datasets. *arXiv preprint arXiv:2512.15110*, 2025.